Fuel Processing Technology 132 (2015) 164–172

Contents lists available at ScienceDirect

Fuel Processing Technology

journal homepage: www.elsevier.com/locate/fuproc

Role of Pt–Pd/γ-Al_2O_3 on the HDS of 4,6-DMBT: Kinetic modeling & contribution analysis

C.O. Castillo-Araiza [a,*], G. Chávez [b], A. Dutta [c], J.A. de los Reyes [b], S. Nuñez [d], J.C. García-Martínez [e]

[a] Grupo de Procesos de Transporte y Reacción en Sistemas Multifásicos, Departamento de IPH, Universidad Autónoma Metropolitana–Iztapalapa, Av. San Rafael Atlixco No. 186, C.P. 09340 México D.F., Mexico
[b] Departamento de IPH, Universidad Autónoma Metropolitana–Iztapalapa, Av. San Rafael Atlixco No. 186, C.P. 09340 México D.F., Mexico
[c] Departement Materiaalkunde, KU Leuven, Kasteelpark Arenberg 44 bus 2450, B-3001 Heverlee-Leuven, Belgium
[d] Facultad de Ciencias Químicas, Universidad Veracruzana, Campus Coatzacoalcos, Coatzacoalcos, Veracruz, Mexico
[e] Departamento de Biofísica, Escuela Nacional de Ciencias Biológicas, IPN, México D.F., Mexico

ARTICLE INFO

Article history:
Received 7 August 2014
Received in revised form 14 December 2014
Accepted 16 December 2014
Available online 15 January 2015

Keywords:
Kinetic modeling
LHHW
Hydrogenation
Desulfurization
Contribution analysis
Pt–Pd/γ-Al_2O_3

ABSTRACT

The purpose of this study is to provide insights on the function of noble metals, namely Pt–Pd catalytic system, on the hydrodesulfurization (HDS) of alkyl-substituted dibenzothiophenes (a-DBTs) by means of kinetic modeling and contribution analyses. A series of Pt–Pd systems (1% wt. nominal loading) supported on γ-Al_2O_3 (0–100, 20–80, 50–50, 80–20 and 100–0; %mol Pt–%mol Pd) are synthesized and evaluated during the HDS of 4,6-dimethyldibenzothiophene (4,6-DMDBT) at operating conditions relevant for industry: 320 °C, 500 ppm of S and an H_2 pressure of 5.5 MPa. A summary of their characterization is presented as reference herein. Kinetic model based on a Langmuir–Hinshelwood–Hougen–Watson (LHHW) mechanism and contribution analysis based on predicted reaction rates give rise to the following findings: the bimetallic catalyst 8Pt–2Pd/γ-Al_2O_3 (80–20; %mol Pt–%mol Pd) leads to the highest activity; in all Pt–Pd/γ-Al_2O_3 systems, Pt favors desulfurization reactions, i.e., 4,6-DMDBT to 3,3′-dimethylphenyl (3,3′-DMBP) and 4,6-dimethyltetrahydrodibenzothiophene (4,6-DM-th-DBT) to MCHT, whereas Pd favors hydrogenation of 4,6-DMDBT to 4,6-DM-th-DBT; and 4,6-DMDBT and methylcyclohexyltoluene (MCHT) are the hydrocarbons with the lowest and highest affinity to be adsorbed on the active sites from the studied Pt–Pd/γ-Al_2O_3 systems, respectively.

1. Introduction

Environmental law for SO_x emission demands reduction of sulfur in transportation fuels. Although the permissive amount of sulfur in diesel amounts to 15 ppm, it is expected to be less than 5 ppm in 2020 [1,2]. Catalytic deep hydrodesulfurization (HDS) is one of the processes used to cope with this environmental regulation [3–6]. Sulfurized CoMo/γ-Al_2O_3 and/or NiMo/γ-Al_2O_3 catalysts are used currently in deep HDS processes [4,7,8]; a complete review of these types of catalysts is presented elsewhere [9–14]. Nevertheless, current catalysts are not sufficiently selective and active to desulfurize alkyl-substituted dibenzothiophenes (a-DBTs) that are recognized to be among the less reactive molecules in treated fuels [2,10,15]. Therefore, both academia and industry are focused on developing more selective and active catalysts for deep HDS of a-DBTs in order to accomplish with the aforementioned sulfur environmental statute [7,16,17].

Particularly, 4,6-DMDBT is used as the main model molecule in most HDS studies since their methyl groups provoke a steric effect that does not favor total desulfurization. Mechanistically, it is well-known that 4,6-DMDBT is desulfurized by either a hydrogenation (HYD) route or a direct desulfurization (DDS) route [4,18]. A group of researches [15, 19–25] proposed that 4,6-DMDBT is adsorbed following π and σ adsorptions: in the former, the aromatic ring of the 4,6-DMDBT is adsorbed on the active site, whereas in the latter the sulfur heteroatom is the one being adsorbed on. It suggests that HYD route involves both π and σ adsorptions while the DSD route involves only σ adsorption. Ho [26] and Prins et al. [15] elucidated that 4,6-DMDBT is kinetically desulfurized through HYD route even at elevated reaction temperatures. Baldovino-Medrano et al. [27] and Chen et al. [28] suggested that the desulfurization of 4,6-DMDBT on noble metals based catalysts is similar for HYD and DDS routes, observing that both routes compete kinetically even when the catalyst active phase contains noble metals. Meriño et al. [23] evaluated bimetallic catalysts based on noble

Abbreviations: HDS, hydrodesulfurization; HYD, hydrogenation; DDS, direct desulfurization; a-DBT, alkyl-substituted dibenzothiophenes; 4,6-DMDBT, 4,6-dimethyldibenzothiophene; 4,6-DM-th-DBT, 4,6-dimethyltetrahydrodibenzothiophene; 3,3′-DMBP, 3,3′-dimethylphenyl; MCHT, methylcyclohexyltoluene; TCD, thermal conductivity detector; FID, flame ionization detector; GC, gas chromatograph; MS, mass spectrometry; TPR, temperature programmed reduction; HR-TEM, high-resolution electron microscopy; FTIR, Fourier transform infrared; LHHW, Langmuir–Hinshelwood–Hougen–Watson; ODEs, ordinary differential equations; RDS, rate-determining steps.

* Corresponding author. Tel.: +52 5558044648.
E-mail address: coca@xanum.uam.mx (C.O. Castillo-Araiza).

http://dx.doi.org/10.1016/j.fuproc.2014.12.028
0378-3820/

metal-molybdenum (NM-Mo/γ-Al_2O_3, NM = Pt, Ru, Pd) during the HDS of dibenzothiophene (DBT), elucidating that the noble metal has a noticeable influence on the reducibility of the sulfide molybdenum phase, favoring the catalytic activity. Yoshimura et al. [29] evaluated monometallic and bimetallic catalysts based on Pd/γ-Al_2O_3, Pt/γ-Al_2O_3, Ru/γ-Al_2O_3 and Rh/γ-Al_2O_3 systems during the HDS of 4,6-DMDBT. The highest activity was obtained from the bimetallic Pt–Pd/γ-Al_2O_3 system, favoring HYD route rather than DDS route, which was, only, related to the synergy of the Pt–Pd hydrogenation properties. Niquille-Röthlisberger and Prins [30] studied Pt/γ-Al_2O_3, Pd/γ-Al_2O_3, and Pt–Pd/γ-Al_2O_3 during the HDS of DBT and 4,6-DMDBT. The bimetallic Pt–Pd system presented the highest activity, which was related to a chemical synergism and the alloy between these noble metals. Jiang et al. [31], Yoshimura et al. [22] and Chen et al. [28] observed that Pd in a Pt–Pd/γ-Al_2O_3 catalyst leads to inhibit Pt agglomeration on the catalyst surface, increasing its hydrogenation activity and its resistance to be deactivated by surface sulfur. Baldovino-Medrano et al. [24] evaluated a silica–alumina supported Pt–Pd catalyst, observing that this bimetallic catalyst is highly active in dibenzothiophene hydrodesulfurization with preferential selectivity to HYD route. Núñez et al. [32] realized oxide-reduction studies for Pt–Pd/TiO_2 and Pt–Pd/γ-Al_2O_3–TiO_2 catalytic systems during the hydrogenation of biphenyl and the HDS of 4,6-DMDBT. Their main results confirmed that the support modifies the physicochemical properties of the Pt–Pd system, i.e., dispersion, acidity, reduction of the active phase, among others. Particularly, the bimetallic Pt–Pd/γ-Al_2O_3 presented the highest activity, related to a synergetic effect due to an adequacy dispersion of Pd on Pt and to the electronic interaction and the alloy between these noble metals.

Most of the studies realized for Pt–Pd catalytic systems have proportioned information on their catalyst performance during the HDS of DBT and a-DBTs, allowing to relate some electronic and superficial properties to their activity and selectivity to HYD and DDS routes. Moreover, there remain some kinetic uncertainties regarding the role of Pt and/or Pd on hydrogenation and desulfurization reactions from HYD route and desulfurization from DDS route. To the best of our knowledge, there are no kinetic studies based on modeling trying to elucidate the role of noble metals during HDS of a-DBTs. As such, the main purpose of this work is to obtain information from a kinetic model of the Pt–Pd system during the HDS of 4,6-DMDBT at operating conditions relevant for industry. Specifically, a series of Pt–Pd/γ-Al_2O_3 (0–100, 20–80, 50–50, 80–20 and 100–0; %mol Pt–%mol Pd) materials are synthesized and a summary of their characterizations obtained from a previous paper [32] is presented as a reference to have a better understanding of the studied catalytic materials. A kinetic model accounting for HYD and DDS routes is developed following Langmuir–Hinshelwood–Hougen–Watson (LHHW) formalism. The model is validated evaluating its phenomenological and statistical reliability. Finally, an analysis of kinetic and adsorption parameters along with a contribution analysis based on the predicted reaction rates is considered to elucidate the kinetic role of monometallic and bimetallic Pt/γ-Al_2O_3, Pt/γ-Al_2O_3 and Pt–Pd/γ-Al_2O_3 catalytic materials on hydrogenation and desulfurization reaction steps.

2. Procedures

2.1. Catalyst

The catalyst support, γ-Al_2O_3, was synthetized by a low-temperature sol–gel method described elsewhere [32]. Nominal molar ratios utilized during support synthesis were 65:20:0.2:1 for alcohol:water:acid:alkoxide, respectively. Aluminum tri-sec-butoxide (Aldrich) and HNO_3 (Baker) were used as organic precursor and hydrolysis catalyst, respectively. Particularly, the alkoxide was mixed together with 2-propanol under vigorous stirring. The obtained alcogel was maintained in maturation for a 24 h period, followed by vacuum drying at a controlled room temperature. Finally, dried gels were held at 120 °C for 1 h, 300 °C for 1 h and then calcined at 500 °C for 2 h.

Supported noble metal materials were synthetized by pore-filling impregnation technique. Noble metal contents was 1% wt. nominal loading. Hexachloroplatinic acid [$H_2PtCl_6 \cdot 6H_2O$] (Aldrich) and palladium nitrate hydrate [$Pd(NO_3)2 \cdot H_2O$] (Aldrich) in aqueous solution were used as precursors. For the case of bimetallic material synthesis, a simultaneous impregnation is carried out. Impregnated solids were dried at 120 °C for 4 h, and annealed at 400 °C for 4 h under static air, wherein the heating ramp was of 1 °C min^{-1}. Finally, calcined materials were reduced at 350 °C under H_2 flow (Praxair, 60 mL min^{-1}, 1 h). Nomenclature used for various catalysts studied in this work is shown in Table 1.

2.1.1. Catalyst properties

As reference for the present kinetic study, characterization results of Pt/γ-Al_2O_3, Pd/γ-Al_2O_3 and Pt–Pd/γ-Al_2O_3 systems obtained by our research group elsewhere [32] are summarized as follows:

(a) γ-Al_2O_3 is a mesoporous material with a superficial area of 374 $m^2 \cdot g^{-1}$, presenting an average pore volume of 0.91 $cm^3 \cdot g^{-1}$ and an average particle diameter of 9.7 nm.
(b) γ-Al_2O_3 is a microcrystalline material with an average particle size in the 3–5 nm range corresponding to aggregated microcrystals.
(c) γ-Al_2O_3 contains essentially Lewis acidity with moderate strength (temperature of desorption ~ 200 °C). The presence of Pt and Pd on the γ-Al_2O_3 has an insignificant effect on textural properties and on the acidity of the γ-Al_2O_3.
(d) γ-Al_2O_3 is not reduced as bimetallic Pt–Pd/γ-Al_2O_3 systems whose reduction is a function of the noble metal composition.
(e) Pt/γ-Al_2O_3 presents oxidic Pt particles with a stronger interaction with the support. Pd/γ-Al_2O_3 reports a decomposition of formed palladium hydride (PdbH) species, suggesting that there is presence of poorly dispersed Pd particles with poor interactions to support. Pd in 8Pt–2Pd/γ-

Table 1
Catalysts' nomenclature and composition considering that noble metal content was 1% wt. nominal loading.

Catalyst/nomenclature	Pt (% mol)	Pd (% mol)
Pt/γ-Al_2O_3	100	0
8Pt–2Pd/γ-Al_2O_3	80	20
5Pt–5Pd/γ-Al_2O_3	50	50
2Pt–8Pd/γ-Al_2O_3	20	80
Pd/γ-Al_2O_3	0	100

Al_2O_3 leads to a better dispersion of Pt and Pd on γ-Al_2O_3 than in metallic and other bimetallic systems suggesting an apparent strong interaction between alloyed Pt and Pd. Besides, Pd in 2Pt–8Pd/γ-Al_2O_3 causes a phase segregation between Pd and Pt on the support.

(f) The metal dispersion for the studied catalytic materials is: 65% in Pt/γ-Al_2O_3; 53% in 8Pt–2Pd/γ-Al_2O_3; 38% in 5Pt–5Pd/γ-Al_2O_3; 35% in 2Pt–8Pd/γ-Al_2O_3; and 30% in Pd/γ-Al_2O_3

2.2. Evaluation

Catalytic systems based on Pt/γ-Al_2O_3, Pd/γ-Al_2O_3 and Pt–Pd/γ-Al_2O_3 are evaluated in kinetic control regime during the HDS of 4,6-DMDBT in a 450 mL stirred batch reactor (Parr 4842) at operating conditions of 320 °C, 5.5 MPa and 1200 rpm (126 rad s^{-1}) mixing speed. The reaction mixture contains 0.2 g of catalyst (materials ex situ reduced at 350 °C under H_2 flow, 60 mL min^{-1}) and 0.2 g of 4,6-DMDBT dissolved in 100 mL of n-dodecane. The runs typically lasted 8 h. Reaction products are analyzed qualitatively by GC–MS (Agilent Technologies 6890N) and quantitatively in a gas chromatograph (GC-FID, Perkin-Elmer Auto System XL) equipped with flame ionization detector and capillary column (5% phenyl–95% methylpolysiloxane, Econo-Cap-5, from Alltech).

2.3. Kinetic model

2.3.1. Reaction scheme

A reaction scheme (see Fig. 1) based on our observations (see Fig. 2 in Section 3.1), and being in agreement with several other investigations [17,33] is used to describe the HDS of 4,6-DMDBT on Pt–Pd/γ-Al_2O_3 catalytic systems. In this reaction scheme HDS of 4,6-DMDBT follows the well-known two HYD and DDS reaction pathways. Methylcyclohexyltoluene (MCHT) and 4,6-dimethyltetrahydrodibenzothiophene (4,6-DM-th-DBT) are all by-products for the HYD route and 3,3′-dimethylphenyl (3,3′-DMBP) without further hydrogenation is the only by-product for the DDS route.

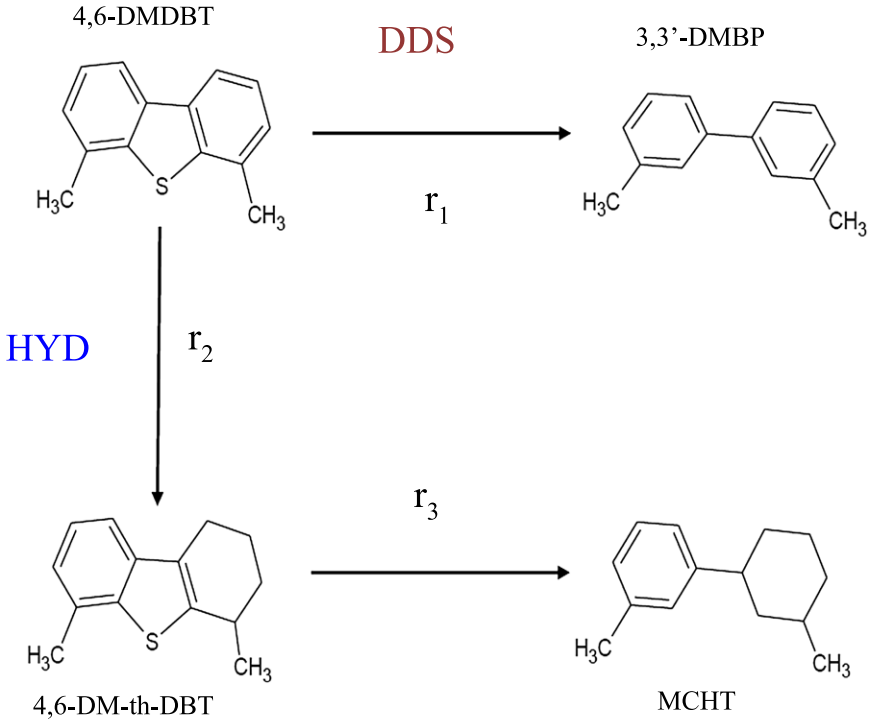

Fig. 1. Reaction scheme for the HDS of 4,6-DMDBT.

2.3.2. Model

It is well known that in the HDS of 4,6-DMDBT, HYD is the preferred reaction pathway, as opposed to DDS because of steric effect caused by the methyl groups in 4,6-DMDBT. Nevertheless, there remain some kinetic uncertainties regarding the role of Pt and/or Pd on hydrogenation and desulfurization reactions from HYD route and desulfurization from DDS route. In this regard, a kinetic model for the HDS of 4,6-DMDBT based on LHHW formalism and pseudo-equilibrium approach is developed to obtain information on the role of Pt/γ-Al_2O_3, Pd/γ-Al_2O_3 and Pt–Pd/γ-Al_2O_3 systems on HYD and DDS routes. The kinetic model for the HDS of 4,6-DMDBT on Pt–Pd/γ-Al_2O_3 system is based on the analysis and results obtained from elsewhere [17], namely hydrocarbons are adsorbed on one type of active sites, which are formed by the presence of coordinatively unsaturated sites (CUS) located at the edges of the catalyst structure, whereas H_2 and H_2S are adsorbed on another type of sites considering the well-known dissociation of H_2S to H and HS. The reliability of the model proposed in this study is evaluated by means of statistical and phenomenological tests as presented later in the text. The reaction mechanism for the HDS of 4,6-DMDBT is presented in Table 2. Molecules such as H, HS and H_2S are considered to be adsorbed on β sites (steps b and f), whereas hydrocarbons such as 4,6-DMDBT, MCHT, 4,6-DM-th-DBT, and 3,3′-DMBP are considered to be adsorbed on σ sites (steps a and c–e). HYD reactions (steps 2 and 3) and DDS reactions (step 1) take place between adsorbed hydrocarbon and adsorbed hydrogen. In Table 2 ν_i is the stoichiometric number in a catalytic cycle describing the reaction route for an overall reaction. Thus, this stoichiometric coefficient indicates the number of times that every adsorption–desorption and/or reaction step has to occur for overall reactions (R_{G1}–

R_{G3}) to take place. Moreover, this stoichiometric number, known as Horiuti number, gives some information about the importance of every adsorption or reaction step (a–f, 1–3) in the catalytic route, i.e., the adsorption of molecular H_2 on β sites (step b) is crucial to both reaction pathways (HYD and DDS) to take place on the catalytic surface.

The kinetic model used to describe the kinetics of HDS of 4,6-DMDBT on Pt–Pd systems supported on γ-Al_2O_3 makes use of Table 2 and is based on the following assumptions:

- Based on experimental studies [34], the presence of intraparticle and interparticle mass transport resistances is negligible, allowing to elucidate the intrinsic kinetics of the catalytic materials evaluated on the routes of HYD and DSD.
- The approximation of pseudo-equilibrium is applied on all steps of adsorption and desorption (a–f). Thus, the mechanism steps accounting for transformations (1–3) are considered as the rate determining steps. Reactions (1–3) are not elementary since they lump intermediate reaction steps that are considered fast enough to be grouped [35].
- Thermodynamics of the global reactions (R_{G1}–R_{G3}) allows considering reaction steps (1–3) as irreversible.
- Pressure of H_2 in gas phase is in excess, and therefore sites β and the concentration of H_2 do not appear in the kinetic model since they are lumped into the kinetic constant of the corresponding reaction rate as discussed elsewhere [17].
- Since the main aim of this study is to relate the kinetic role of a series of Pt/γ-Al_2O_3, Pd/γ-Al_2O_3 and Pt–Pd/γ-Al_2O_3 systems on HYD and DDS routes during the HDS of 4,6-DMDBT, the heats of adsorption and activation energies are not analyzed here, but they need to be accounted for in future studies wherein experiments at different temperatures are mandatory.

Based on the aforementioned, the kinetic model can be written as follows:

$$r_1 = k_1 C_{4,6DMDBT} \theta_\sigma \tag{1}$$

$$r_2 = k_2 C_{4,6DMDBT} \theta_\sigma \tag{2}$$

$$r_3 = k_3 C_{4,6DM-th-DBT} \theta_\sigma \tag{3}$$

$$\theta_\sigma = 1 - \theta_{4,6DMDBT} - \theta_{3,3'DMBP} - \theta_{4,6DM-th-DBT} - \theta_{MCHT} \tag{4}$$

where the fractions of intermediate species on active phase (σ) involved during the reaction are given as:

$$\theta_{4,6DMDBT} = \frac{K_{4,6DMDBT} C_{4,6DMDBT}}{1 + K_{4,6DMDBT} C_{4,6DMDBT} + K_{3,3'DMBP} C_{3,3'DMBP} + K_{4,6DM-th-DBT} C_{4,6DM-th-DBT} + K_{MCHT} C_{MCHT}} \tag{5}$$

$$\theta_{3,3'DMBP} = \frac{K_{3,3'DMBP} C_{3,3'DMBP}}{1 + K_{4,6DMDBT} C_{4,6DMDBT} + K_{3,3'DMBP} C_{3,3'DMBP} + K_{4,6DM-th-DBT} C_{4,6DM-th-DBT} + K_{MCHT} C_{MCHT}} \tag{6}$$

$$\theta_{4,6DM-th-DBT} = \frac{K_{4,6DM-th-DBT} C_{4,6DM-th-DBT}}{1 + K_{4,6DMDBT} C_{4,6DMDBT} + K_{3,3'DMBP} C_{3,3'DMBP} + K_{4,6DM-th-DBT} C_{4,6DM-th-DBT} + K_{MCHT} C_{MCHT}} \tag{7}$$

$$\theta_{MCHT} = \frac{K_{MCHT} C_{MCHT}}{1 + K_{4,6DMDBT} C_{4,6DMDBT} + K_{3,3'DMBP} C_{3,3'DMBP} + K_{4,6DM-th-DBT} C_{4,6DM-th-DBT} + K_{MCHT} C_{MCHT}}. \tag{8}$$

The model describing the concentration of different compounds observed in the batch reactor is given as:

$$\frac{dC_n}{dt} = \sum_i^n v_n r_i, \tag{9}$$

with initial conditions:

$$C_n = C_{no,} \text{ when } t = 0. \tag{10}$$

Kinetic parameters are estimated by minimizing a weighted objective function RSS (β), which includes the residual sum of squares of the concentration of the different species:

$$RSS(\beta) = \sum_{n=1}^{n_{resp}} W_n \sum_{k=1}^{n_{resp}} \left(C_{k,n} - \hat{C}_{k,n} \right)^2 \xrightarrow{\beta_1, \beta_2, \ldots\ldots, \beta_n} \min \tag{11}$$

where β is optimal parameter vector, n_{exp} is the number of independent experiments, n_{resp} is the number of responses, $C_{k,n}$ and $\hat{C}_{k,n}$ are the n-th experimental and predicted responses, respectively for the k-th observation, and w_n is the weight factor assigned to the n-th response.

The reactor model is described by a system of ordinary differential equations (ODEs), see Eqs. (1)–(10). The subroutine VODE was used to solve the corresponding set of ODEs [36]. The initial minimization of the objective function (Eq. (11)) in the model regression is carried out

using the Rosenbrock method [37]. Then the ODRPACK subroutine is used for fitting calculated values to the corresponding experimental data points [38]. This set of subroutines can perform either weighted orthogonal regression or nonlinear least squares for explicit and implicit models using multi-response data with an implementation of the Levenberg-Marquardt method [39] obtaining an estimation of 95% confidence interval. The F-test for the global significance of the regression as well as the individual *t*-test and the confidence limits for the estimates were computed. Apart from this, the correlation between pairs of estimated parameters was accounted for by computing the so-called binary linear correlation coefficients (ρ_{ij}). When the value of ρ_{ij} is close to ± 1, a strong linear relationship between the estimated parameters i and j occurs.

2.4. Contribution analysis

A contribution analysis of the various reactions considered in the model is carried out. This methodology accounts for the effect of rate kinetic coefficients, adsorption coefficients and reactant concentration since integral contribution factors are determined by using the predicted reaction rates integrated over time. These factors allow quantifying the relative importance of the different reactions considered in our reaction scheme and mechanism since these are used to develop our kinetic model presented in Section 2.3. The contribution factor is given as follows:

$$\varphi_{i,j} = \frac{r_{ij}}{\sum_i rij.} \tag{12}$$

The integral contribution factor $\varphi_{i,j}$ of the elementary step i toward the appearance/disappearance of component j is defined as the ratio of the rate of appearance/disappearance of j resulting from reaction i, r_{ij} to the total rate of appearance/disappearance of j inside the reactor.

3. Results and discussion

Section 3.1 discusses catalytic observation in terms of conversion and concentration of the different components observed during the HDS of 4,6-DMDBT on the evaluated catalytic systems. Section 3.2 presents the results of the kinetic model in terms of an analysis of the fitted catalytic observations and estimated parameters. Finally, Section 3.3 discusses the integral calculated contribution factors for the observed compounds analyzing their role on the HYD and DDS pathways.

3.1. Evaluation analysis

Fig. 2 shows experimental results obtained when monometallic Pt/γ-Al_2O_3 and Pd/γ-Al_2O_3 systems and bimetallic Pt–Pd/γ-Al_2O_3 systems are evaluated. Fig. 2a depicts observed conversion of 4,6-DMDBT as function of time. As reported in literature [27,31,40], monometallic Pt/γ-Al_2O_3 system leads to a higher conversion than Pd/γ-Al_2O_3 system, but bimetallic Pt–Pd/γ-Al_2O_3 catalysts present a higher conversion than monometallic ones. In bimetallic Pt–Pd/γ-Al_2O_3 systems, activity increases as the contents of Pt increase, being the 8Pt–2Pd/γ-Al_2O_3 the most active catalyst among the evaluated materials. Fig. 2b presents the concentration integrated over time of HDS reaction products (4,6-DM-th-DBT, MCHT and 3,3′-DMBP) for the different Pt–Pd/γ-Al_2O_3 catalytic systems. From these concentration trends, 4,6-DMDBT reacts essentially through the HYD route producing 4,6-DM-th-DBT that in turns reacts to form MCHT. As expected 4,6-DMDBT reacts in a minor way to produce 3,3′-DMBP through DDS route because of steric hindrance caused by methyl groups in this sulfur molecule. As Pd content increases, hydrogenation of 4,6-DMDBT to 4,6-DM-th-DBT is favored over desulfurization of both 4,6-DM-th-DBT and 4,6-DMDBT that produce MCHT and 3,3′-DMBP, respectively. The bimetallic Pt–Pd/γ-Al_2O_3 catalyst exhibits a higher selectivity to desulfurize products than monometallic catalytic systems. In fact, Pd/γ-Al_2O_3 system exhibits the highest production of 4,6-DM-th-DBT but the lowest production of MCHT and 3,3′-DMBP. Further Pt/γ-Al_2O_3 presents opposite results, avoring mainly desulfurization of 4,6-DM-th-DBT and 4,6-DMDBT rather than hydrogenation of the latter molecule. Among the bimetallic systems, the catalytic properties of the 8Pt–2Pd/γ-Al_2O_3 system prompted the highest desulfurization of 4,6-DMDBT through both HYD and DDS routes. Thus, hydrogenation properties related to the greater dispersion of Pt and Pd in 8Pt–2Pd/γ-Al_2O_3 along with the alloy and electronic synergy in this catalytic system [32] are fundamental aspects to improve Pt–Pd interaction and, hence, desulfurization of 4,6-DMDBT. Besides, the lowest activity of the Pd/γ-Al_2O_3 in comparison to Pt/γ-Al_2O_3 catalytic system is apparently related to the decomposition of formed palladium hydride (PdbH) species and, hence, to the poor dispersion of Pd on γ-Al_2O_3.

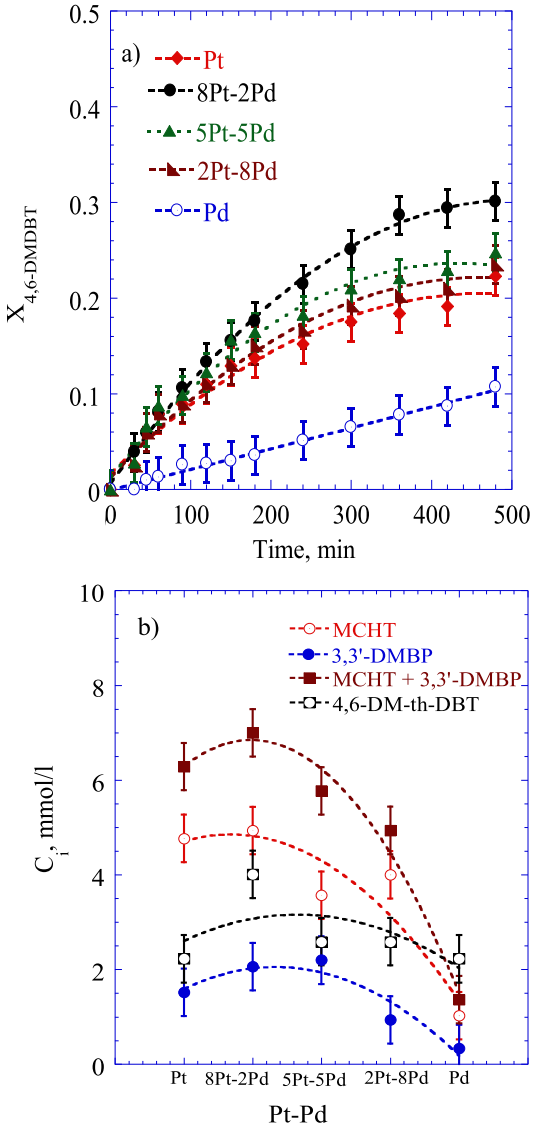

Fig. 2. Observations during the HDS of 4,6-DMDBT on Pt–Pd/γAl_2O_3 systems: a) Conversion of 4,6-DMDBT as a function of time; and b) Concentration of reaction products integrated over time.

Table 2
Reaction mechanism for the HDS of 4,6-DMDBT on Pt–Pd/γ-Al_2O_3.

Step	Mechanism based on LHHW formalism	υ_1	υ_2	υ_3
a	$4,6-DMDBT+\sigma \rightleftharpoons 4,6-DMDBT\sigma$	1	1	1
b	$H_2+2\beta \rightleftharpoons 2H\beta$	2	2	5
1	$4,6-DMDBT\sigma+4H\beta \rightleftharpoons 3,3'-DMBP\sigma+2\beta+H\beta+SH\beta$	1	0	0
2	$4,6-DMDBT\sigma+4H\beta \rightleftharpoons 4,6-DM-th-DBT\sigma+4\beta$	0	1	1
3	$4,6-DM-th-DBT\sigma+6H\beta \rightleftharpoons MCHT\sigma+4\beta+H\beta+SH\beta$	0	0	1
c	$3,3'-DMBP\sigma \rightleftharpoons 3,3'-DMBP+\sigma$	1	0	0
d	$4,6-DM-th-DBT\sigma \rightleftharpoons 4,6-DM-th-DBT+\sigma_1$	0	1	1
e	$MCHT\sigma \rightleftharpoons MCHT+\sigma$	0	0	1
f	$H\beta+SH\beta \rightleftharpoons H_2S+2\beta$	1	0	1
R_{G1}	$4,6-DMDBT+2H_2 \rightleftharpoons 3,3'-DMBP+H_2S$	1	0	0
R_{G2}	$4,6-DMDBT+2H_2 \rightleftharpoons 4,6-DM-th-DBT$	0	1	0
R_{G3}	$4,6-DM-th-DBT+3H_2 \rightleftharpoons MCHT+H_2S$	0	0	1

3.2. Kinetic analysis

Even though the models are developed for five Pt–Pd/γ-Al_2O_3 catalytic systems, the performances of Pt/γ-Al_2O_3, 8Pt–2Pd/γ-Al_2O_3 and Pd/γ-Al_2O_3 are analyzed in this study since these materials contain information necessary to elucidate the kinetic role of the monometallic and bimetallic studied noble metals. Fig. 3 depicts a comparison between fitted and observed conversions and observed concentration profiles of 4,6-DMDBT and reaction products (3,3′-DMBP, MCHT and 4,6-DM-th-DBT) as a function of time during the HDS reaction on the aforementioned selected catalysts. The model fits adequately the experimental observations. The estimated parameters are presented in Table 3. Both regression and parameters are statistically significant according to: (a) the F-value obtained (648–1162) compared to the F-value tabulated (3.01); (b) interval of confidence of each parameter; and (c) linear correlation coefficients (ρ_{ij}) are around ±0.8 indicating a weak linear relationship between pair of estimated parameters. Therefore, a phenomenological analysis of estimated parameters and kinetic expressions can be carried out with reliability.

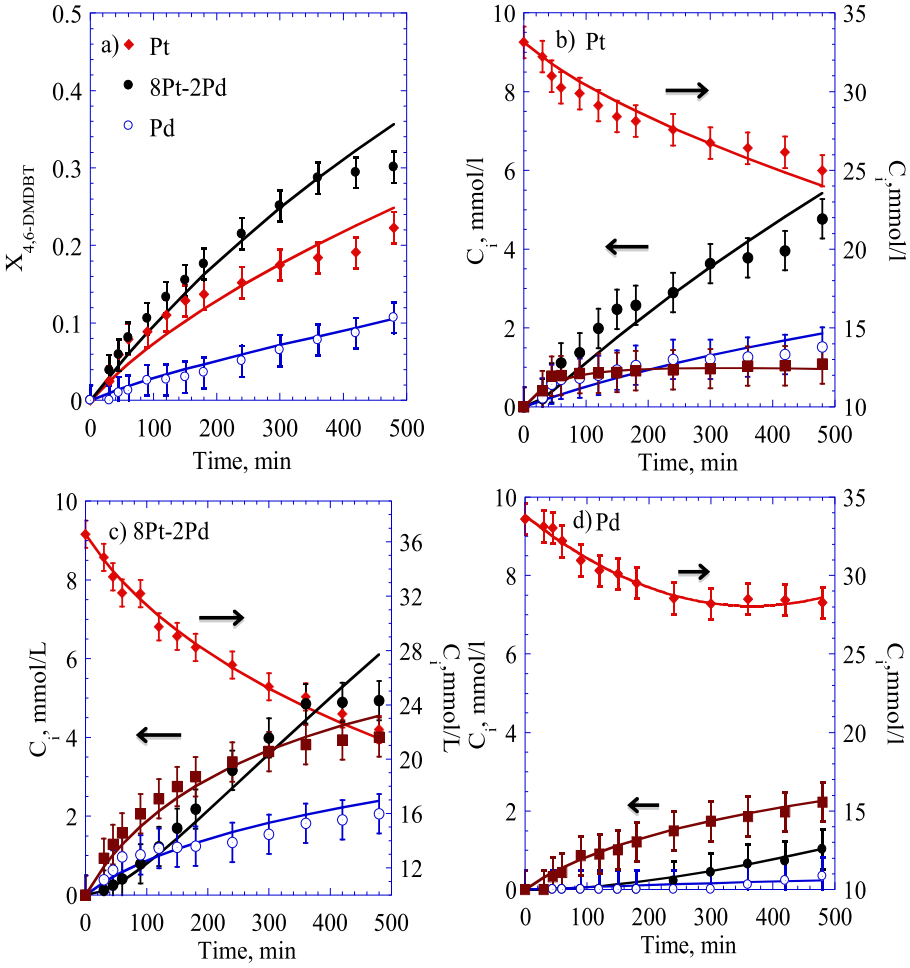

Fig. 3. Model fit. (a) Conversion of 4,6-DMDBT as a function of time. Product concentration profiles as function of time for: (b) Pt/γ-Al_2O_3, (c) 8Pt–2Pd/γ-Al_2O_3 and (d) Pd/γ-Al_2O_3 systems. Symbols represent observations and full lines the model fitting. In Figs. (b)–(d): (♦) $C_{4,6\text{-DMDBT}}$, (○) $C_{3,3\text{-DMBF}}$, (■) $C_{4,6\text{-DM-th-DBT}}$ (•) C_{MCHT}.

Table 3
Estimated kinetic parameters.

Parameter	Pd/γ-Al_2O	8Pt–2Pd/γ-Al_2O_3	Pt/γ-Al_2O_3
k1 (min^{-1})/10^{-5}	1.7 ± 0.04	46 ± 1.9	27.5 ± 2.3
k2 (min^{-1})/10^{-4}	2.6 ± 0.06	20.6 ± 0.72	11.6 ± 0.3
k3 (min^{-1})/10^{-3}	1.9 ± 0.04	13.2 ± 0.73	24.1 ± 2.6
K4,6DMDBT (L/mmol)/10^{-5}	5.4 ± 0.16	0.04 ± 0.01	48.7 ± 1.2
KMCHT (L/mmol)/10^{-1}	7.2 ± 5.0	40.2 ± 8.1	33.7 ± 6.5
K3,3DMBP (L/mmol)/10^{-1}	1.9 ± 0.61	2 ± 0.06	2.1 ± 0.06
K4,6DM-th-DBT (L/mmol)/10^{-1}	1.2 ± 0.02	1.2 ± 0.06	1.3 ± 0.4
F-value[a]	648	1109	1162

a Statistics: Ftab = 3.01 for 1 − α = 0.95 with 10 degrees of freedom.

Although a contribution analysis based on integrated reaction rates is, strictly speaking, required to determine in quantitative terms the relative importance of the various steps in the reaction scheme, see Fig. 1, the magnitude order of the relative estimated kinetic parameters can provide a preliminary idea of how HYD and DDS pathways occur during the HDS of 4,6-DMDBT. As expected steric effect related to the methyl groups of the 4,6-DMDBT leads mainly to the formation of 4,6-DM-th-DBT via HYD route than to 3,3′-DMBP via DDS route, [5,17,41,42], since the reaction rate coefficient k_2 is larger than k_1. Besides, the catalyst activity to form MCHT (k_3) is the highest one since $k_3 > k_2 > k_1$, indicating that once the 4,6-DM-th-DBT is formed its desulfurization to MCHT is kinetically favorable as corroborated on the contribution analysis further. On the other hand, adsorption constants follow the next trend: $K_{MCHT} \gg K_{3,3'DMBP} > K_{4,6\text{-}DMthDBT} \gg K_{4,6\text{-}DMDBT}$. These results are different to those reported for industrial catalysts such as CoMo/γ-Al_2O_3 and/or NiMo/γ-Al_2O_3 systems wherein the 4,6-DMDBT is the hydrocarbon with the highest affinity to be adsorbed on the catalytic active phase, i.e., $K_{4,6\text{-}DMDBT} > K_{MCHT} \approx K_{4,6DMthDBT} \approx K_{3,3'DMBF}$ [17]. Therefore, the adsorption constants obtained for the Pt–Pd/γ-Al_2O_3 systems suggest a strong affinity of MCHT on σ active sites, inhibiting after a period of reaction time when its concentration is highly considerable both in HYD and DDS reaction pathways. In fact it is observed on catalyst evaluation that after 500 min of reaction, a pseudo stationary state is identified even when there is a high concentration of 4,6-DMDBT to be consumed on the reaction atmosphere, a result that is not observed when industrial catalysts are evaluated, where total conversion of 4,6-DMDBT is achieved at similar operating conditions [5,17,43].

To facilitate the comparison of kinetic performances of noble metals, namely Pt/γ-Al_2O_3, 8Pt–2Pd/γ-Al_2O_3 and Pd/γ-Al_2O_3 catalysts, relative kinetic parameters referenced to catalyst Pd/γ-Al_2O_3 have been calculated via information presented in Table 3. Furthermore, relative parameters for Pt/γ-Al_2O_3, 8Pt–2Pd/γ-Al_2O_3 and Pd/γ-Al_2O_3 systems are presented in Table 4. The analysis of these parameters allows to elucidate the kinetic effect of each of the noble metals on the HDS of 4,6-DMDBT, which has roughly been discussed from the qualitative analysis of the raw experimental data in the previous section. Relative reaction rate coefficients related to hydrogenation of 4,6-DMDBT via HYD route (k_1/k_{1ref}) and desulfurization of 4,6-DMDBT via DDS route (k_2/k_{2ref}), show that 8Pt–2Pd/γ-Al_2O_3 system favors the reaction of 4,6-DMDBT via HYD and DDS routes since this material presents the highest activity in terms of the relative coefficients obtaining values of $k_1/k_{1ref} = 27$ and $k_2/k_{2ref} = 7.9$. Pt/γ-Al_2O_3 system presents a moderate activity, obtaining values of $k_1/k_{1ref} = 16.1$ and $k_2/k_{2ref} = 4.5$ while Pd/γ-Al_2O_3 system presents the lowest activity, being the referenced catalyst, i.e., $k_1/k_{1ref} = 1$ and $k_2/k_{2ref} = 1$. Nevertheless, the Pt/γ-Al_2O_3 catalyst shows the highest activity to desulfurize 4,6-DM-th-DBT to MCHT, obtaining a value of $k_3/k_{3ref} = 12.5$. 8Pt–2Pd/γ-Al_2O_3 and Pd/γ-Al_2O_3 systems present values of $k_3/k_{3ref} = 6.8$ and $k_3/k_{3ref} = 1$, respectively. On the other hand, the relative constants of adsorption (K_i/K_{iref}) indicate that 3,3-′DMBP and 4,6-DM-th-DBT have similar affinity to be adsorbed on active sites σ from the three studied catalytic systems. MCHT presents similar affinity to be adsorbed on catalytic systems presenting Pt, being higher than on those systems presenting Pd on active phase; and the adsorption of 4,6-DMDBT is totally different in the evaluated catalytic systems, obtaining the highest affinity to be adsorbed on the catalytic site σ from Pt/γ-Al_2O_3 system and the lowest affinity on active sites σ from 8Pt–2Pd/γ-Al_2O_3 system.

3.3. Contribution analysis

Integral contribution factors are determined by using the reaction rates integrated over time through Eq. (12) allowing to quantify the importance of each of the global reaction steps. As stated above, contribution factors do account for the effects of both kinetic and adsorption parameters and reactant concentration. Table 5 presents integrated reaction rates and contribution factors obtained for three catalytic systems: Pt/γ-Al_2O_3, 8Pt–2Pd/γ-Al_2O_3 and Pd/γ-Al_2O_3, considered as references to infer kinetic information of the noble metals and their interaction on the HDS of 4,6-DMDBT. An analysis of reaction rates points out that Pd/γ-Al_2O_3 system favors reactions in HYD route and Pt/γ-Al_2O_3 system favors reactions in DDS route. Besides, the synergy of noble metals elucidated in 8Pt–2Pd/γ-Al_2O_3 system shows preference for both DDS and HYD routes.

Besides, the contribution analysis indicates the following findings: (a) when Pd/γ-Al_2O_3 system is evaluated hydrogenation of 4,6-DMDBT to 4,6-DM-th-DBT ($\varphi = 89\%$) via HYD route is favored in comparison to its desulfurization to 3,3′-DMBP ($\varphi = 11\%$) via DDS route; (b) Pt/γ-Al_2O_3 system presents opposite results being the desulfurization of 4,6-DMDBT ($\varphi = 96\%$) via DDS route preferred with respect to its hydrogenation to 4,6-DM-th-DBT ($\varphi = 4\%$) via HYD route. The electronic synergy and greater dispersion of these noble metals in the best catalytic system (8Pt–2Pd/γ-Al_2O_3) lead to selectively favor both the hydrogenation of 4,6-DMDBT to 4,6-DM-th-DBT ($\varphi = 64\%$) via HYD route and its desulfurization to 3,3′-DMBP ($\varphi = 32\%$) via DDS route compared to those monometallic systems as apparently observed from the reaction rate values integrated over time, see Table 5. Integral contribution factors also provide information on the desulfurization of 4,6-DM-th-DBT to MCHT via HYD route, wherein the largest contribution factors are for those catalysts containing Pt in their active phase, 8Pt–2Pd/γ-Al_2O_3 ($\varphi = 68\%$) and Pt/γ-Al_2O_3 ($\varphi = 99\%$) systems, with

Table 4
Relative kinetic parameters referenced to Pd/γ-Al_2O_3 catalytic system.

Parameter	Pd/γ-Al_2O	8Pt–2Pd/γ-Al_2O_3	Pt/γ-Al_2O_3
k1/k1,cat1	1.0	27.0	16.1
k2/k2,cat1	1.0	7.9	4.5
k3/k3,cat1	1.0	6.8	12.5
K4,6DMDBT/K4,6DMDBT,cat1	1.0	0.01	9.0
KMCHT/KMCHT,cat1	1.0	5.6	4.6
K3,3DMBP/K3,3DMBP,cat1	1.0	1.1	1.1
K4,6DM-th-DBT/K4,6DM-th-DBT,cat1	1.0	1.0	1.1

Table 5
Reaction rates integrated over time and integral contribution factors.

Parameter	Pd/γ-Al_2O_3	8Pt–2Pd/γ-Al_2O_3	Pt/γ-Al_2O
$R_{4,6\text{-}DMDBT,\ HYD}$ mmol/(kg of cat s)/10^{-1}	1.38	2.56	0.05
$R_{4,6DMDBT,DDS}$ mmol/(kg of cat s)/10^{-1}	0.17	1.47	1.35
$R_{4,6\text{-}DMDBT,\ HYD}/R_{4,6\text{-}DMDBT,\ DDS}$	8.10	1.74	0.04
$\varphi_{4,6\ -\ DMDBT,1}$	11	36	96
$\varphi_{4,6\ -\ DMDBT,2}$	89	64	4
$\varphi_{4,6\ -\ DMthDBT,2}$	59	32	1
$\varphi_{4,6\ -\ DMthDBT,3}$	41	68	99

respect to that Pd/γ-Al_2O_3 ($\varphi = 41\%$) catalyst. Hence, Pt essentially favors the desulfurization of 4,6-DM-th-DBT. This is in agreement with the catalyst evaluation: catalysts containing a higher concentration of Pd lead to higher productions of 4,6-DM-th-DBT compared to those observed for 3,3-′DMBP and MCHT, see Fig. 2b, whereas catalysts containing a higher concentration of Pt cause a higher production of 3,3-′DMBP and MCHT compared to the production of 4,6-DM-th-DBT.

4. Conclusions

Compared to the studies reported in literature for Pt–Pd systems on catalyst performance during the HDS of a-DBTs, the kinetic modeling and contribution analysis carried out in this work allow to identify the main character of Pt and Pd in both hydrogenation and desulfurization reactions from HYD and DDS pathways. The main findings are summarized as follows: (1) 4,6-DMDBT is the hydrocarbon with the lowest affinity to be adsorbed on active sites whereas MCHT, once produced via the desulfurization of 4,6-DM-th-DBT, is the hydrocarbon with the highest affinity to be adsorbed on active sites; (2) Pd essentially favors hydrogenation of 4,6-DMDBT to 4,6-DM-th-DBT, whereas Pt favors desulfurization reactions to produce MCHT via HYD route and 3,3-′DMBP via DDS route. These results become relevant since they, along with catalyst characterization, are the basis to propose a new catalyst design using noble metals for deep HDS in future investigations.

Nomenclature

Roman letters

av	specific external surface area, $m^2 \cdot m^{-3}$
C_n	concentration of component n, $mmol \cdot kg^{-1}$
k_n	reaction rate coefficient, h^{-1}
K_n	adsorption equilibrium coefficient for component n, Pa^{-1}
r_n	reaction rate of reaction n, $mmol \cdot (m^3 \cdot h^{-1})$
R_g	universal gas constant, $kJ \cdot (mol \cdot K)^{-1}$
R_n	net reaction rate of the component n, $mmol \cdot (g \cdot h)^{-1}$
RSS	objective function
w_n	objective function weight factor of each response
W	mass of catalyst, g

Greek letters

β_i	vector of parameters accounted for in the objective function
θ_σ	fraction coverage of vacant sites
θ_n	fraction coverage of component n
$\varphi_{i,j}$	integral contribution factor of the elementary step i toward the appearance/disappearance of component j
β, σ	active sites on LHHW mechanism
ρ	density, $kg \cdot m^3$
ν_i	Horiuti number in Table 2

Subscripts

exp	experiment
f	fluid
g	gas phase
hc	hydrocarbon
n	component n
obs	observed
p	particle
r	response
ref	reference
s	surface

Superscripts

^	calculated

Acknowledgments

The authors would like to thank the two anonymous reviewers (especially the first reviewer) for their helpful and constructive comments that greatly contributed to improving the final version of the manuscript.

References

[1] NOM-086-SEMARNAT-SENER-SCFI, Secretary, E.S. Environment and Natural Resources Secretary, 2006, p. 18.
[2] N. Azizi, S.A. Ali, K. Alhooshani, T. Kim, Y. Lee, J.-I. Park, Hydrotreating of light cycle oil over NiMo and CoMo catalysts with different supports, Fuel Processing Technology 109 (2013) 172–178.
[3] H. Topsøe, Hydrotreating catalysis: from molecular understanding to improved industrial solutions, ACS National Meeting Book of Abstracts, Haldor Topsøe A/S, Nymøllevej 55, DK-2800 Kgs, Lyngby, Denmark, 2009.
[4] M. Breysse, G. Djega-Mariadassou, S. Pessayre, C. Geantet, M. Vrinat, G. Pérot, Deep desulfurization: reactions, catalysts and technological challenges, Catalysis Today 84 (2003) 129–138.
[5] M.L. Vrinat, The kinetics of the hydrodesulfurization process — a review, Applied Catalysis 6 (1983) 137–158.
[6] Y. Sun, H. Wang, R. Prins, Hydrodesulfurization with classic Co-MoS_2 and Ni-MoS_2/γ-Al_2O_3 and new Pt–Pd on mesoporous zeolite catalysts, Catalysis Today 150 (2010) 213–217.
[7] K. Shimada, Y. Yoshimura, Ultra-deep hydrodesulfurization and aromatics hydrogenation of diesel fuel over a Pd–Pt catalyst supported on yttrium-modified USY, Journal of the Japan Petroleum Institue 46 (2003) 368–374.
[8] J. Ancheyta, G.F. Froment, Y. Sun, H. Wang, R. Prins, Hydrodesulfurization with classic Co-MoS_2 and Ni-MoS_2/γ-Al_2O_3 and new Pt–Pd on mesoporous zeolite catalysts, Catalysis Today 150 (2010) 213–217.
[9] P. Grange, X. Vanhaeren, Hydrotreating catalysts, an old story with new challenges, Catalysis Today 36 (1997) 375–391.
[10] C. Song, An overview of new approaches to deep desulfurization for ultra-clean gasoline, diesel fuel and jet fuel, Catalysis Today 86 (2003) 211–263.
[11] M. Vrinat, R. Bacaud, D. Laurenti, M. Cattenot, N. Escalona, S. Gamez, New trends in the concept of catalytic sites over sulfide catalysts, Catalysis Today 107–108 (2005) 570–577.
[12] J. Shen, G. Shi, Progress of Catalysts for Deep Hydrodesulfurization of Fuels, Shiyou Huagong/Petrochemical Technology372008. 1111–1120.
[13] T. Kabe, W. Qian, Y. Hirai, L. Li, A. Ishihara, Hydrodesulfurization and hydrogenation reactions on noble metal catalysts, Journal Catalysis 190 (2000) 191–198.
[14] J.M. Campos-Martin, S. Rojas, S.T. Oyama, T. Gott, H. Zhao, Y.-K. Lee, Transition metal phosphide hydroprocessing catalysts: a review, Catalysis Today 143 (2009) 94–107.
[15] R. Prins, M. Egorova, A. Roethlisberger, Deep hydrodesulfurization on Ni-MoS_2, Co-MoS_2, and Pt–Pd catalysts on Al_2O_3 and ASA, Abstracts of Papers 229th ACS National Meeting, San Diego, CA, United States March 1317 2005, 2005 (p. FUEL–140).
[16] M. Egorova, R. Prins, Hydrodesulfurization of dibenzothiophene and 4,6-dimethyldibenzothiophene over sulfided NiMo/γ-Al_2O_3, CoMo/γ-Al_2O_3, and Mo/γ-Al_2O_3 catalysts, Journal Catal. 225 (2004) 417–427.
[17] J.C. García-Martínez, C.O. Castillo-Araiza, J.A. de Los Reyes Heredia, Trejo, A. Montesinos, Kinetics of HDS and of the inhibitory effect of quinoline on HDS of 4,6-DMDBT over a Ni–Mo–P/Al_2O_3 catalyst: part I, Chemical Engineering Journal 210 (2012) 53–62.
[18] Y. Zhao, N. Sivasankar, P. Kukula, R. Prins, M. Egorova, A. Ro, Mechanisms of hydrodesulfurization and hydrodenitrogenation, 1112006. 84–93.
[19] H. Zhu, X. Lu, W. Guo, L. Li, L. Zhao, H. Shan, Theoretical insight into the desulfurization of thiophene on Pt(110): a density functional investigation, Journal Molecular Catalysis A Chemical 363 (2012) 18–25.
[20] K. Herbst, M. Brorson, A. Carlsson, Hydrotreating activities of alumina-supported bimetallic catalysts derived from noble metal containing molecular sulfide clusters Mo_3S_4M' (M′ = Ru, Rh, Ir, Pd, Pt), Journal Molecular Catalysis A Chemical 325 (2010) 1–7.
[21] I.R. Galindo, J.A. de los Reyes, Effect of alumina–titania supports on the activity of Pd, Pt and bimetallic Pd–Pt catalysts for hydrorefining applications, Fuel Processing Technology 88 (2007) 859–863.
[22] Y. Yoshimura, M. Toba, T. Matsui, M. Harada, Y. Ichihashi, K.K. Bando, Active phases and sulfur tolerance of bimetallic Pd–Pt catalysts used for hydrotreatment, Applied Catalysis A General 322 (2007) 152–171.
[23] L.I. Meriño, A. Centeno, S.A. Giraldo, Influence of the activation conditions of bimetallic catalysts NM-Mo/γ-Al_2O_3 (NM = Pt, Pd and Ru) on the activity in HDT reactions, Applied Catalysis A General 197 (2000) 61–68.
[24] V.G. Baldovino-Medrano, S.A. Giraldo, A. Centeno, Highly HYD selective Pd–Pt/support hydrotreating catalysts for the high pressure desulfurization of DBT type molecules, Catalysis Letters 130 (2009) 291–295.
[25] B. Pawelec, R. Mariscal, R. Navarro, S. van Bokhorst, S. Rojas, J.L. Fierro, Hydrogenation of aromatics over supported Pt–Pd catalysts, Applied Catalysis A General 225 (2002) 223–237.
[26] T.C. Ho, Deep HDS, of diesel fuel: chemistry and catalysis, Catalysis Today 98 (2004) 3–18.
[27] V.G. Baldovino-Medrano, P. Eloy, E.M. Gaigneaux, S.A. Giraldo, A. Centeno, Development of the HYD route of hydrodesulfurization of dibenzothiophenes over Pd–Pt/γ-Al_2O_3 catalysis, Journal Catalysis 267 (2009) 129–139.

[28] S. Chen, J. Chen, R. Gieleciak, C. Fairbridge, Reactivity characteristics of Pt-encapsulated zeolite catalysts for hydrogenation and hydrodesulfurization, Applied Catalysis A General 415–416 (2012) 70–79.
[29] Y. Yoshimura, M. Toba, H. Farag, K. Sakanishi, Ultra deep hydrodesulfurization of gas oils over sulfide and/or noble metal catalysts, Catalysis Surveys Japan 8 (2004) 47–60.
[30] A. Niquille-Röthlisberger, R. Prins, Hydrodesulfurization of 4,6-dimethyldibenzothiophene and dibenzothiophene over alumina-supported Pt, Pd, and Pt–Pd catalysts, 242 (2006) 207–216.
[31] H. Jiang, H. Yang, R. Hawkins, Z. Ring, Effect of palladium on sulfur resistance in Pt–Pd bimetallic catalysts, Catalysis. Today 125 (2007) 282–290.
[32] S. Núñez, J. Escobar, A. Vázquez, J.A. de los Reyes, M. Hernández-Barrera, 4,6-Dimethyl-dibenzothiophene conversion over Al_2O_3–TiO_2-supported noble metal catalysts, Materials Chemistry Physics 126 (2011) 237–247.
[33] A. Niquille-Röthlisberger, R. Prins, Hydrodesulfurization of 4,6-dimethyldibenzothiophene and dibenzothiophene over alumina-supported Pt, Pd, and Pt–Pd catalysts, Journal Catalysis 242 (2006) 207–216.
[34] L. Alvarado-Perea, I.R. Galindo-Esquivel, E.S. Perez-Cisneros, J.A. de Los Reyes Heredia, T. Viveros, The effect of solvent on the kinetics and mass transfer resistances for 4,6 DMDBT HDS, Int. Journal Chemical Reactor Engineering 3 (2005).
[35] G.B. Marin, G.S. Yablonsky, Kinetics of Complex Reactions, Wiley-VCH, Decoding Complexity, Germany, 2011. 428.
[36] P.N. Brown, G.D. Byrne, A.C. Hindmarsh, VODE: a variable-coefficient ODE solver, Journal Scientific Statistical Computing 10 (1989) 1038–1051.
[37] H.H. Rosenbrock, An automatic method for finding the greatest or least value of a function, Computer Journal 3 (1960) 175–184.
[38] P.T. Boggs, J.R. Donaldson, R.H. Byrd, R.B. Schnabel, Algorithm 676 ODRPACK: software for weighted orthogonal distance regression, ACM Transactions Mathematical Software 15 (1989) 348–364.
[39] D.W. Marquardt, An algorithm for least-squares estimation of nonlinear parameters, Journal Society Industrial Applied Mathematics 11 (1963) 431–441.
[40] R.M. Rioux, T.J. Toops, W.N. Delgass, A. Niquille-Röthlisberger, R. Prins, Hydrodesulfurization of 4,6-dimethyldibenzothiophene over Pt, Pd, and Pt–Pd catalysts supported on amorphous silica–alumina, Catalysis Today 123 (2007) 198–207.
[41] S. Pessayre, C. Geantet, R. Bacaud, M. Vrinat, T.S. N'Guyen, Y. Soldo, et al., Platinum doped hydrotreating catalysts for deep hydrodesulfurization of diesel fuels, Industrial Engineering Chemistry Research 46 (2007) 3877–3883.
[42] B. Delmon, G.F. Froment, P. Grange, H.R. Reinhoudt, R. Troost, A.D. van Langeveld, Testing and characterisation of Pt/ASA and PtPd/ASA for deep HDS reactions, Studies Surface Science Catalysis 127 (1999) 251–258.
[43] V. Vanrysselberghe, R.L. Gall, G.F. Froment, Hydrodesulfurization of 4-methyldibenzothiophene and 4,6-dimethyldibenzothiophene on a $CoMo/Al_2O_3$ catalyst: reaction network and kinetics, Industrial Engineering Chemistry Research 37 (1998) 1235–1242.